Assessment of Realizability Constraints and Boundary Conditions in $\overline{v^2} - f$ Turbulence Models

A. Sveningsson and L. Davidson

Department of Thermo and Fluid Dynamics, Chalmers University of Technology,

SE-412 96 Gothenburg, Sweden

Abstract — In this study a two-dimensional stator vane passage flow and the fully developed channel flow (Re=395) are computed. Two different $\overline{v^2} - f$ turbulence models [1], [2] are used. Focus is on the use of the realizability constraint on the turbulent time scale originally suggested by Durbin [3]. It is shown that this time scale bound is inconsistent in farfield regions and it is argued that the bound should not be used in the equation for the relaxation parameter, f. In this equation the constraint acts as to increase the wall-normal Reynolds stress component $\overline{v^2}$ and also to cause numerical problems. In these computations the stator vane test case is used to demonstrate the effect the constraint has in different terms in the turbulence model. Finally, some comments are made about the wall boundary conditions for ε and f. Two different implementations, which give identical results, are used for the channel flow.

1. Introduction

During the last few years the $\overline{v^2} - f$ turbulence model, originally suggested by Durbin, has become increasingly popular due to its ability to correctly account for near-wall damping without use of damping functions. The $\overline{v^2} - f$ model has also shown to be superior to other RANS methods in many fluid flows where complex flow features are present. In this study the behaviour of two versions of the $\overline{v^2} - f$ model are compared in an attempt to investigate in what aspects they differ and also to improve the overall understanding of $\overline{v^2} - f$ models' performance.

The test cases used in this study are a fully developed channel flow and a stagnation point linear cascade flow. With the strong blockage in the latter flow it is crucial to handle the overprediction of turbulent kinetic energy upstream the stator vane. This is done by use of the Durbin time scale bound. The central part of this work is an assessment of the use of this bound, especially in the f equation, which is shown to be inconsistent in some cases.

2. Governing Equations

The steady RANS equations read

$$U_j \frac{\partial U_i}{\partial x_j} = -\frac{1}{\rho}\frac{\partial P}{\partial x_i} + \nu \frac{\partial^2 U_i}{\partial x_j^2} - \frac{\partial}{\partial x_j}\overline{u_i u_j}, \qquad \frac{\partial U_j}{\partial x_j} = 0 \tag{1}$$

The unknown Reynolds stresses are closed using the eddy-viscosity concept, i.e.

$$\overline{u_i u_j} = -2\nu_t S_{ij} + \frac{2}{3}k\delta_{ij}; \;\; \nu_t = C_\mu \overline{v^2}\mathcal{T}, \;\; \text{where } \mathcal{T} = \max\left(\frac{k}{\varepsilon}, 6\sqrt{\frac{\nu}{\varepsilon}}\right) \tag{2}$$

The turbulent quantities k and ε are governed by transport equations that read

$$u_j \frac{\partial k}{\partial x_j} = \frac{\partial}{\partial x_j}\left(\left(\nu + \frac{\nu_t}{\sigma_k}\right)\frac{\partial k}{\partial x_j}\right) + P_k - \varepsilon \tag{3}$$

$$u_j \frac{\partial \varepsilon}{\partial x_j} = \frac{\partial}{\partial x_j}\left(\left(\nu + \frac{\nu_t}{\sigma_\varepsilon}\right)\frac{\partial \varepsilon}{\partial x_j}\right) + \frac{C_{\varepsilon 1}P_k - C_{\varepsilon 2}\varepsilon}{\mathcal{T}} \tag{4}$$

Model	C_μ	$C_{\varepsilon d}$	$C_{\varepsilon 2}$	C_1	C_2	σ_k	σ_ε	C_L	C_η
1 [4]	0.22	0.045	1.9	1.4	0.3	1.0	1.3	0.25	85
2 [2]	0.19	0.045	1.9	0.4	0.3	1.0	1.3	0.23	70
2 [5]	0.22	0.05	1.9	0.4	0.3	1.0	1.3	0.23	70

Table 1: $\overline{v^2} - f$ model constants

In this work the performance of two different $\overline{v^2} - f$ models have been compared. They will hereafter be referred to as Model 1 and Model 2, respectively. In Model 1, given in Parneix et al. [4], the wall-normal Reynolds stress component, $\overline{v^2}$, is modelled using

$$u_j \frac{\partial \overline{v^2}}{\partial x_j} = \frac{\partial}{\partial x_j}\left(\left(\nu + \frac{\nu_t}{\sigma_k}\right)\frac{\partial \overline{v^2}}{\partial x_j}\right) + kf - \frac{\overline{v^2}}{k}\varepsilon \tag{5}$$

$$L^2 \frac{\partial^2 f}{\partial x_j^2} - f = \frac{C_1 - 1}{\mathcal{T}}\left(\frac{\overline{v^2}}{k} - \frac{2}{3}\right) - C_2\frac{P_k}{k} \tag{6}$$

The turbulent length scale, L, and the modified coefficient $C_{\varepsilon 1}$ are calculated using

$$L = C_L \max\left(\frac{k^{3/2}}{\varepsilon}, C_\eta \frac{\nu^{3/4}}{\varepsilon^{1/4}}\right), \quad C_{\varepsilon 1} = 1.4\left(1 + C_{\varepsilon d}\sqrt{k/\overline{v^2}}\right) \tag{7}$$

Unfortunately, the wall boundary conditions for the dissipation rate, ε, and the redistribution parameter, f,

$$\varepsilon \to 2\nu\left(\frac{k}{y^2}\right); \quad f \to \frac{-20\nu^2}{\varepsilon}\left(\frac{\overline{v^2}}{y^4}\right) \quad \text{as} \ y \to 0 \tag{8}$$

make the original formulation somewhat unstable. The slight modification to Model 1 used in e.g. Kalitzin [2] and Lien and Kalitzin [5] solves this problem and renders the following $\overline{v^2}$ and f equations (Model 2)

$$u_j \frac{\partial \overline{v^2}}{\partial x_j} = \frac{\partial}{\partial x_j}\left(\left(\nu + \frac{\nu_t}{\sigma_k}\right)\frac{\partial \overline{v^2}}{\partial x_j}\right) + kf - 6\overline{v^2}\frac{\varepsilon}{k} \tag{9}$$

$$L^2 \frac{\partial^2 f}{\partial x_j^2} - f = \frac{C_1}{\mathcal{T}}\left(\frac{\overline{v^2}}{k} - \frac{2}{3}\right) - C_2\frac{P_k}{k} - 5\frac{\overline{v^2}}{k\mathcal{T}} \tag{10}$$

with a Dirichlet f boundary condition. Note that the models given in Lien and Kalitzin [5] and Kalitzin [2] only differ in model constant values, cf. Table 1. For a more thorough discussion on the differences between the above models consult Sveningsson [6].

2.1. The Realizability Constraint

Most eddy viscosity based turbulence models overpredict the turbulent kinetic energy (TKE) in stagnation point flows. Durbin [3] suggested a bound on the turbulent time scale, $\mathcal{T}$, derived from $2k \geq \overline{u^2} \geq 0$, which significantly improves TKE predictions. For $\overline{v^2}$-f models this constraint implies

$$\mathcal{T} = \min\left(\max\left(\frac{k}{\varepsilon}, 6\sqrt{\frac{\nu}{\varepsilon}}\right), \frac{C_{lim}k}{3C_\mu \overline{v^2}}\frac{1}{\max \lambda_\alpha}\right) \tag{11}$$

586

where the constant C_{lim} has been added to allow for tuning against experiments and $\max \lambda_\alpha$ is the largest eigenvalue of the strain rate tensor S_{ij}. The mechanism responsible for the improvement in TKE predictions is the reduction in modelled production rate of TKE

$$P_k = 2C_\mu \overline{v^2} \mathcal{T} S_{ij} S_{ij} \tag{12}$$

2.2. On the Use of Realizability Constraints in the $\overline{v^2} - f$ Model

In order to illustrate the effect of realizability rewrite the f equation (Eqn. 10)

$$0 = \frac{C_2 P_k}{L^2 k} + \frac{1}{\mathcal{T} L^2} \left[(5 - C_1) \frac{\overline{v^2}}{k} + \frac{2}{3} C_1 \right] - \frac{f}{L^2} + \frac{\partial^2 f}{\partial x_j^2} \tag{13}$$

The first two terms are source terms ($C_1 = 0.4$), the third act as a sink whereas the last term is a diffusive term. Now imagine our time scale limiter being active. This means that P_k/k in the first source term initially will decrease (as P_k will affect k it is not obvious whether the quantity P_k/k at a later stage will actually decrease or increase). This decrease will to some extent be balanced by an increase of the second source term as this term is multiplied by $1/\mathcal{T}$. Since the objective of the limit of $\mathcal{T}$ is to reduce k (and ν_t) this countereffect is incorrect as kf forms the source term in the $\overline{v^2}$ equation.

From inspection of Eqn. 11, we see that the possible increase of $\overline{v^2}$ further reduces the time scale $\mathcal{T}$. This positive feedback has caused some of the stator vane computations to diverge as f becomes increasingly larger. Note that the f equation is of elliptic nature and that any perturbation is felt in the entire computational domain. The easiest way to get around this problem is to not use the time scale limit at all in the f equation. Another possible route is to rewrite the realizability constraint in terms of $\overline{v^2}/k < C_{lim}/(3C_\mu \mathcal{T} \max \lambda_\alpha)$ for the f equation, which consistently lowers the $\overline{v^2}$ part of the turbulent kinetic energy. Finally, [5] suggested a similar bound on the turbulent length scale L appearing in the f equation, which has also been investigated.

2.2.1. The Consequence of Realizability in the Farfield

In the farfield the elliptic operator $\partial^2 f/\partial x_j^2$ is assumed to be negligible (in fact, [7] showed that this is not the case even for fully developed channel flow) and the f equation of Model 2 reduces to

$$-f = \frac{C_1}{\mathcal{T}} \left(\frac{\overline{v^2}}{k} - \frac{2}{3} \right) - C_2 \frac{P_k}{k} - 5 \frac{\overline{v^2}}{k \mathcal{T}} \tag{14}$$

With this expression for f the $\overline{v^2}$ equation source term in Eqn. 9 becomes

$$-\frac{C_1}{\mathcal{T}} \left(\overline{v^2} - \frac{2}{3} k \right) + C_2 P_k + 5 \frac{\overline{v^2}}{\mathcal{T}} - 6 \frac{\overline{v^2}}{k} \varepsilon \tag{15}$$

Now assume we have an isotropic flow ($\overline{v^2} = 2k/3$), in which the production of TKE is negligible. We get

$$+\frac{10k}{3\mathcal{T}} - \frac{12}{3} \varepsilon \tag{16}$$

587

which yields the correct isotropic dissipation rate $-2\varepsilon/3$ when $\mathcal{T} = k/\varepsilon$. But when the flow approaches a stagnation region the value of $\mathcal{T}$ becomes smaller than k/ε (or $\varepsilon < k/\mathcal{T}$) as the time scale bound is activated (cf. Figure 5(b)). As already mentioned the time scale bound ought to decrease $\overline{v^2}$ but clearly, from Eqn. 16, it will cause a physically incorrect production of $\overline{v^2}$. And, as this production increases $\overline{v^2}$, it further restrains the time scale bound (Eqn. 11). Note that this inconsistency is six times larger in Model 2 than in Model 1. This feedback can also cause numerical problems. The obvious solution to this anomaly is to not use the realizability constraint in the f equation or to change the modelled $\overline{v^2}$ dissipation rate according to

$$\varepsilon_{\overline{v^2}} = -6\frac{\overline{v^2}}{\mathcal{T}} \tag{17}$$

One of these modifications proved to be necessary in order to achieve a converged solution with Model 2 for the stator vane computations where the stagnation region indeed is very large.

3. Some Comments on Wall Boundary Conditions

In the literature there are some inconsistencies concerning the implementation of non-zero wall boundary conditions in $\overline{v^2} - f$ models, e.g. $\varepsilon \to 2\nu k/y^2$. Usually this condition is imposed on the first interior node to enforce the correct behaviour of ε. The other alternative is to specify this limit *on* the wall.

Using Taylor expansion it can readily be shown that the nearwall behaviour of k and ε are

$$k = \frac{1}{2}(\overline{a_1^2} + \overline{c_1^2})y^2 + \mathcal{O}(y^3) \qquad \varepsilon = \nu\left(\overline{a_1^2} + \overline{c_1^2}\right) + \mathcal{O}(y) \tag{18}$$

For small values of y the higher order terms can be neglected which means that ε approaches a *constant* value of $2\nu k/y^2$ and that this value can be used as boundary condition for ε by specifing this limit *on* the wall node (but evaluated at the first interior node). However, in literature the most common way to implement this type of boundary condition is to specify this limit at the first interior node via source terms. For the two formulations to be equivalent ε must be constant for y^+ values lower than the y^+ value of the first node, which typically is of order 1. In Figure 1(a) the ε profiles from DNS data and the three $\overline{v^2} - f$ models are plotted for $0 < y^+ < 5$. Clearly, the assumption of ε being constant for $y^+ \leq 1$ can be questioned. However, both implementations of the ε boundary condition give the same result indicating that it is unimportant whether boundary conditions like Eqn. 8 are specified on the boundary or at the first interior node.

4. Solver

CALC-BFC (Boundary Fitted Coordinates) is a structured code using the pressure correction scheme SIMPLEC and a co-located grid arrangement with Rhie and Chow interpolation. The van Leer scheme was used when discretizising the momentum and turbulence equations. Due to convergence problems false time-stepping was used to enhance the numerical stability. The momentum equations where solved with a segregated Tri-Diagonal Matrix Solver (TDMA) and the turbulence equations where solved with either a segregated or coupled [6] (Model 1) TDMA.

5. Results

5.1. 1-D Channel Flow

From the channel flow computations it was seen that the differences in results between the $\overline{v^2} - f$ models were small. The profile differing the most was the $\overline{v^2}$ profile shown in Figure 1(b). For a closer comparison see [6].
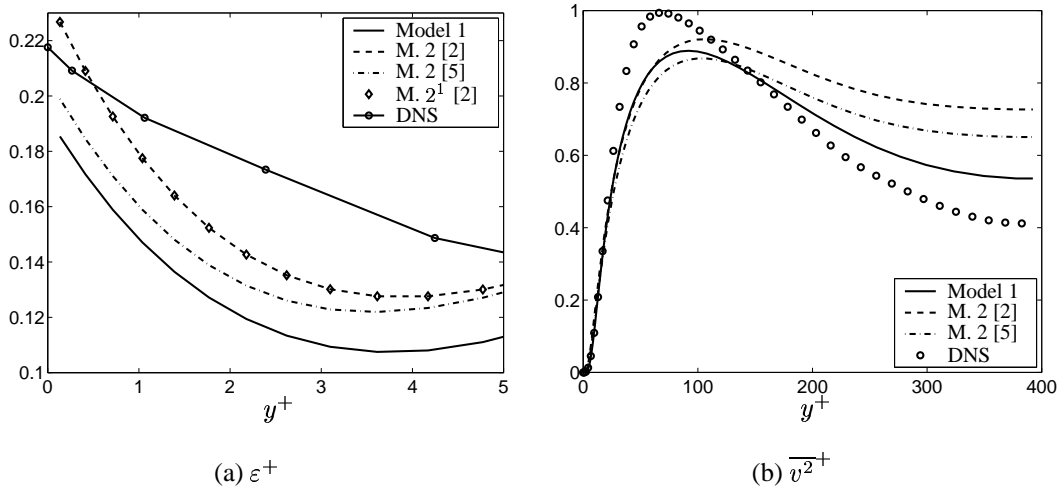
Figure 1: 1-D channel flow. a) Near-wall dissipation rate for the two models (two sets of constants for Model 2) using two different implementations of the ε wall boundary condition. [1]) Boundary condition specified *on* the wall. b) Wall-normal Reynolds stress for the two models.

5.2. The Effect of the Realizability Constraint in a Stagnation Point Flow

In order to illustrate the importance of the realizability constraint contours of k/U_{in}^2 for the stator vane flow are shown in Figure 2. In all three cases the same $\overline{v^2} - f$ model, Model 1, has been used with the only difference that in Figure 2(a) the realizability constraint, Eqn. 11, is deactivated, in Figure 2(b) the constraint is used when calculating ν_t and in the ε equation, whereas in Figure 2(c) it has been used everywhere the time scale $\mathcal{T}$ appears. It can be seen that the constraint has a strong influence. For example, when the limiter is active, it is only in a narrow region around the wake that k/U_{in}^2 exceeds levels of 10^{-3}, whereas the same quantity is well above this value in almost the entire domain if the constraint is not used.

As $\mathcal{T}$ appears in several terms in the equations governing the $\overline{v^2} - f$ model it would be interesting to find out in which terms the effect of a limitation of $\mathcal{T}$ is the strongest. Clearly, from comparison of Figures 2(b) and 2(c) showing almost identical results, it must be the use of the time scale bound in the expression for ν_t that prevents the turbulent kinetic energy from taking erroneous values. Use of the bound also in the f equation seems to have little effect on the solution as Figures 2(b) and 2(c) are almost identical. In order to make a quantitative comparison of the effect realizability has on the k distribution k/U_{in}^2 is plotted along the stagnation line in Figure 3. All these computations are carried out using Model 1. The combinations are all listed in Table 2.

In Figure 3(a) the importance of using the time scale bound is again obvious. The k profile obtained without the bound has a maximum about 30 times higher than the maximum of any other profile. The influence of C_{lim} is also illustrated. In Figure 3(b) it can be seen that the use of the realizability constraint (in terms of $\mathcal{T}$, or L) in the f equation has only little influence on k. The profile standing out is from the computation where the time scale bound has only been used in the ν_t expression. Hence, it can be concluded that the use of the bound in the f equation is not important, that using it in the ε equation *increases* k (i.e. k is lower without the bound, cf. Figure 3(b)) and that the only reason that the constraint works is the limitation of the turbulent viscosity.
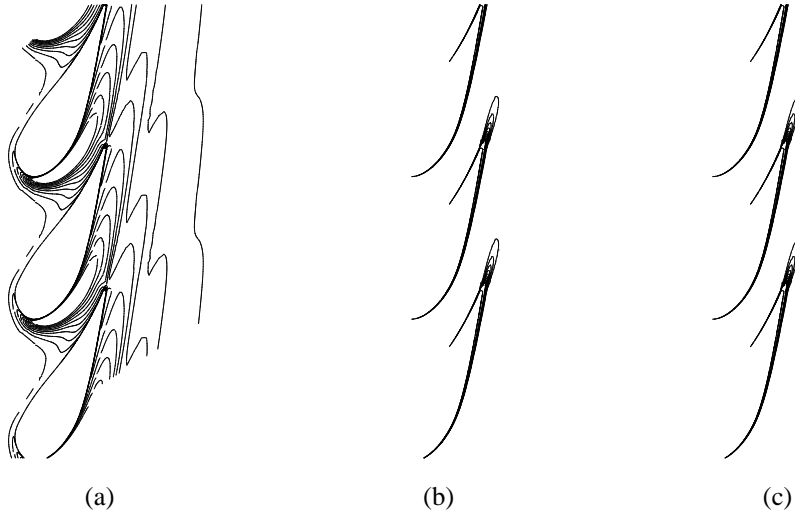
589

(a)   (b)   (c)

Figure 2: Contours of k/U_{in}^2. Inlet flow from left. (a) Case A; (b) Case C; (c) Case E. Contour intervals of 0.003, 0.001 and 0.001, respectively.

Case	Description
A	No realizability constraint
B	Constraint on $\mathcal{T}$ used in ν_t ($C_{lim} = 0.6$)
C	Constraint on $\mathcal{T}$ used in ν_t and ε equation
D	Constraint on $\mathcal{T}$ used in ν_t, ε and f equations
E	Constraint on $\mathcal{T}$ and L used in ν_t, ε and f equations
F	Same as E but with $C_{lim} = 1.0$
G	Same as E but modified $\overline{v^2}$ dissipation rate (cf. Eqn. 17)

Table 2: Description of how realizability is used when investigating its influence in the stagnation region.
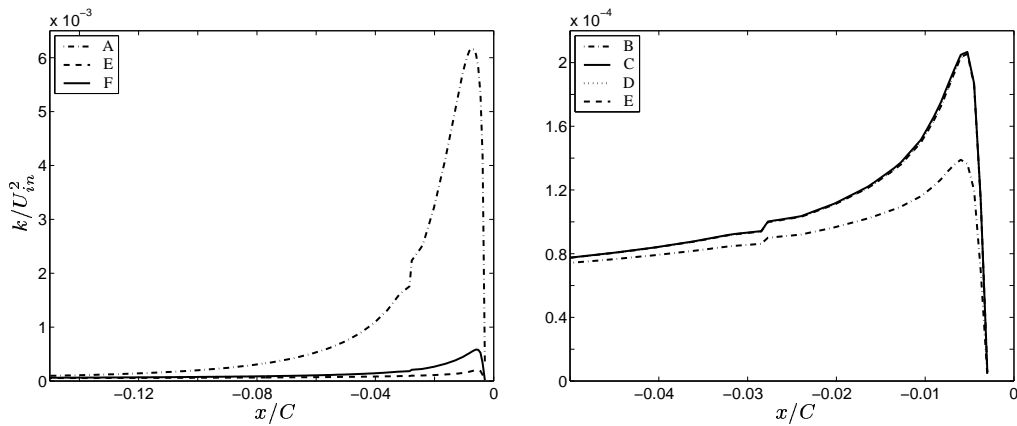

Figure 3: Profiles of k/U_{in}^2 approaching the stagnation point for different realizability constraints. For legend see Table 2. Left: Global view. Right: Close-up.
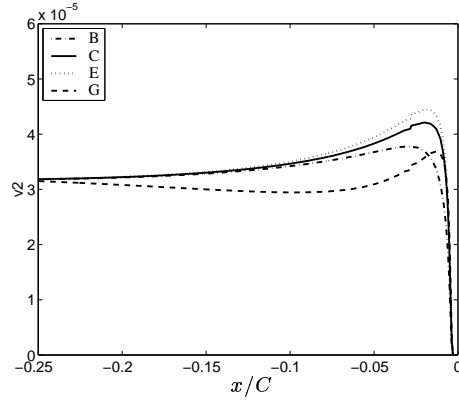
Figure 4: Profiles of $\overline{v^2}/U_{in}^2$ approaching the stagnation point for different realizability constraints. For legend see Table 2.

For the $\overline{v^2}$ profiles along the stagnation line the differences are somewhat larger. In Figure 4 profiles of the normalized wall normal Reynolds stress component, $\overline{v^2}/U_{in}^2$, are shown. We see that Case B, consistent with the lower values of k in Figure 3(b), gives lower values than Cases C and E (D gave the same results as E, i.e. there seems to be no effect of the realizability constraint on the turbulent length scale, L, suggested in [5]). The other profile that stands out is the G profile. In Case G the ratio ε/k in the $\overline{v^2}$ equation has been replaced with $\mathcal{T}^{-1}$ as was suggested in Section 2.2.1. The modification was introduced in order to have the correct farfield limiting behaviour in regions where the realizability constraint is active. As can be seen this change decreases the value of $\overline{v^2}$ in the region upstream the stator vane. Another effect of this change is that close to solid walls the other time scale bound expressed in Kolmogorov variables, $\mathcal{T} > 6\sqrt{\nu/\varepsilon}$, modifies the modelled dissipation rate in the $\overline{v^2}$ equation. To be more precise, this makes the $\overline{v^2}$ dissipation rate behave as y^4 instead of y^2 as $y \to 0$. This has two implications. Firstly, it will change the near-wall behaviour of $\overline{v^2}$. Secondly, the reduced dissipation rate of $\overline{v^2}$, i.e. an increase in $\overline{v^2}$, seems to improve the numerical stability of the $\overline{v^2} - f$ model.

Finally, the influence of the realizability constraint on the turbulent viscosity, ν_t, is investigated. In Figure 5 the profiles of normalized turbulent viscosity ν_t/ν along the stagnation line are shown. Just as for the other turbulent quantities the constraint has a remarkable effect on ν_t. As soon as the presence of the vane makes the flow decelerate (or accelerate) the eigenvalues of the strain rate tensor, S_{ij}, becomes large enough to activate the time scale constraint (cf. Eqn. 11). In Figure 5(b) contours of the ratio $(k/\varepsilon)/\mathcal{T}$ are shown. They indicate in which regions the time scale constraint is active and to what extent the turbulence time scale is modified. Wherever the ratio is greater than unity, which is almost the entire vane passage, the realizability constraint is active. This means that the turbulence model is modified in most of the domain. For example, the eddy viscosity in the active regions is given by $\nu_t = C_{lim}k/(3\max\lambda_\alpha)$, which is very different from the original ν_t expression. This suggests that the choice of the constant C_{lim} becomes rather important in stagnation point flows and that the original ν_t expression severely overestimates the eddy viscosity. Note that the physically justified lowest value of C_{lim} is unity, whereas a value of 0.6 has been used in Figure 5(b). As the active region is large the lower value might cause a too strong bound on the turbulent time scale.

6. Conclusions

The use of the realizability constraint in $\overline{v^2} - f$ turbulence models has been assessed by computing a two-dimensional stator vane flow. In this flow the stagnation region is large and it was
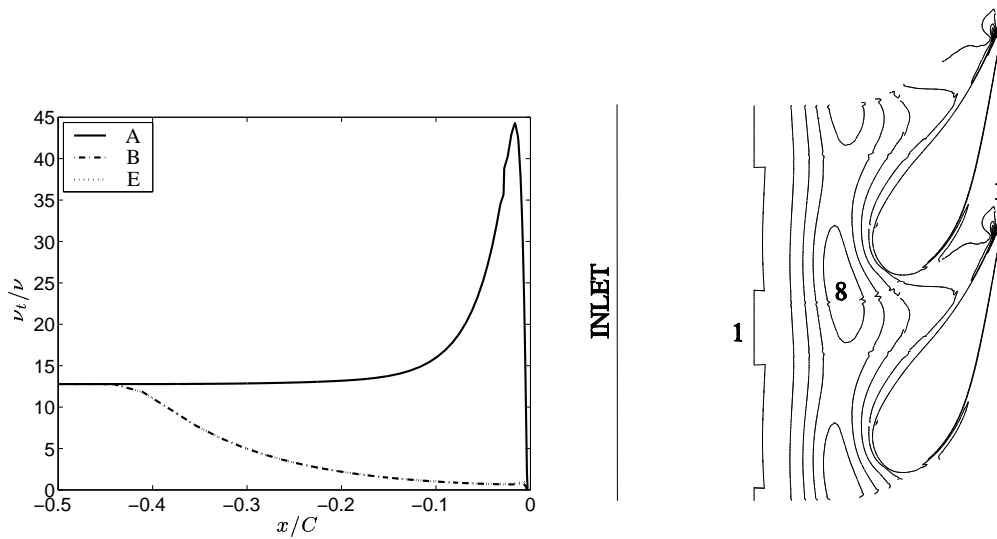
Figure 5: Left: Profiles of ν_t/ν approaching the stagnation point for different realizability constraints. For legend see Table 2. Right: Contours of $(k/\varepsilon)/\mathcal{T}$ at midspan indicating in which areas the time scale constraint is active. For values above 1 the constraint is active.

found that using the constraint when calculating the eddy-viscosity was necessary in order to prevent an unphysical growth of turbulent kinetic energy. It was also shown that the standard use of the realizability constraint in the $\overline{v^2} - f$ model is inconsistent and some modifications that solved the problem were suggested. Further, it was found that the constraint in the f equation has little influence on the final solution. However, using the constraint in this equation can cause numerical problems. Finally, two different implementations of the ε and f wall boundary condition were used. Both gave identical results.

7. Acknowledgement

References

1. S. Parneix and P.A. Durbin. Numerical simulation of 3d turbulent boundary layers using the $\overline{v^2} - f$ model. Center for Turbulence Research Annual Research Breifs, 1997.
2. G. Kalitzin. Application of the $\overline{v^2} - f$ model to aerospace configurations. Center for Turbulence Research Annual Research Breifs, 1999.
3. P.A. Durbin. On the k-3 stagnation point anomaly. *International Journal of Heat and Fluid Flow*, 17:89–90, 1995.
4. S. Parneix, P.A. Durbin, and M. Behnia. Computation of 3-d turbulent boundary layers using the v2f model. *Flow, Turbulence and Combustion*, 60:19–46, 1998.
5. F.S. Lien and G. Kalitzin. Computations of transonic flow with the $\overline{v^2}$-f turbulence model. *International Journal of Heat and Fluid Flow*, 22:53–61, 2001.
6. A. Sveningsson. Analysis of the performacne of different $\overline{v^2} - f$ turbulence models in a stator vane passage flow. Licentiate thesis, Dept. of Thermo and Fluid Dynamics, Chalmers University of Technology, Gothenburg, 2003.
7. Lars Davidson, Peter V. Nielsen, and A. Sveningsson. Modifications of the $v^2 - f$ model for computing the flow in a 3d wall jet. In *4th Int. Symp. on Turbulence Heat and Mass Transfer*, Antalya, Turkey, 2003.